

## Condensed phase of liquid $^4\text{He}$

P. M. Lam and M. L. Ristig

*Institut für Theoretische Physik,*

*Universität zu Köln, 5 Köln 41, Germany*

(Received 25 July 1978)

The long-range order of the one- and two-body density matrices is analyzed for the ground state of liquid  $^4\text{He}$  described by suitable Jastrow wave functions  $\Psi = \prod_{i<j} f(r_{ij})$ . The condensate fraction, pairing function, pairing energy, and related quantities are calculated as functions of density. The evaluations are performed within the diagrammatic formalism developed by Ristig and Clark. For the most part we employ the optimal correlation functions  $f(r)$  and associated radial distribution functions  $g(r)$ . Both quantities are determined self-consistently by performing a paired-phonon analysis. The numerical treatment is based on the hypernetted-chain procedure for the structure function as well as for the one-body density matrix. The condensate fraction is found to be 0.113 at the experimental equilibrium value of the particle density, and shrinks to a value  $\sim 0.05$  at densities in the solidification region of  $^4\text{He}$ . The pairing functions show remarkable intermediate structure. The pairing energy is negative, about  $-50$  mK at saturation density, and increases rapidly with increasing density. It changes sign at a density close to the experimental melting point. It is found that the condensate fraction depends only weakly on temperature in the range of temperatures considered.

### I. INTRODUCTION

It is generally believed that it is the long-range coherence of the many-body system which may account for the macroscopic quantum properties of liquid  $^4\text{He}$  associated with superfluidity. F. London suggested an intimate relationship between the superfluid density and Bose-Einstein condensation which may occur in liquid  $^4\text{He}$  below the  $\lambda$  point.<sup>1</sup> The connection, however, has not been rigorously established. The subject still remains an intriguing question of fundamental interest.<sup>2,3</sup>

To clarify the possible role of the Bose-Einstein condensate we shall concentrate in this study on a detailed numerical exploration of the successive density matrices. These quantities permit a complete description of liquid  $^4\text{He}$ , particularly, its long-range order.<sup>4,5</sup>

A plausible general form for the exact ground-state wave function of a system of  $A$  interacting bosons is<sup>6</sup>

$$\begin{aligned} \Psi_0(\vec{r}_1, \vec{r}_2, \vec{r}_3, \dots, \vec{r}_A) \\ = \prod_{i<j}^A f(r_{ij}) \prod_{i<j<k}^A f_3(\vec{r}_i, \vec{r}_j, \vec{r}_k) \\ \times \prod_{i<j<k<l}^A f_4(\vec{r}_i, \vec{r}_j, \vec{r}_k, \vec{r}_l) \cdots \quad (1) \end{aligned}$$

It appears that a satisfactory first approximation to the wave function (1) for liquid  $^4\text{He}$  is the Bijl-

### Dingle-Jastrow function<sup>7</sup>

$$\Psi(\vec{r}_1, \vec{r}_2, \dots, \vec{r}_A) = \prod_{i<j}^A f(r_{ij}), \quad (2)$$

where  $f(r)$  is a two-body correlation factor with  $f(r) \rightarrow 1$  as  $r \rightarrow \infty$  and appropriate behavior at distance  $r=0$ . In a following step of systematic approximation scheme we could improve upon Ansatz (2) by including the triple correlation factor  $f_3$ , etc.<sup>8</sup>

It has been demonstrated for wave function (2) that the zero-momentum single-particle orbital is macroscopically occupied.<sup>9,10</sup> Ansatz (2) therefore cannot shed much light on a possible absence of a single-particle condensate.<sup>11</sup> To explore such a situation it might be necessary to adopt a differing approximation procedure<sup>2</sup> to take proper account of those contributions which are distributed among all correlation factors  $f_3, f_4, \dots, f_A$ . Here, we ignore this possibility and assume the presence of a macroscopic Bose condensate in liquid  $^4\text{He}$ . We adopt further Ansatz (2) to describe the ground state.

A very substantial and productive effort has gone into a detailed study of the form (2) and its consequences. Particularly the liquid structure function and the optimal radial distribution function have been the objects of numerous studies in correlated wave-function theory.<sup>2,3,12,13</sup>

In recent years interest has been focused also on the exploration and enumeration of the one- and two-body density matrices of quantum fluids. These

quantities are defined at zero temperature by

$$\langle \bar{r}_1 | \Gamma_1 | \bar{r}_1' \rangle = \frac{A}{N} \int \Psi^*(\bar{r}_1, \bar{r}_2, \dots, \bar{r}_A) \Psi(\bar{r}_1', \bar{r}_2, \dots, \bar{r}_A) dr_2 \cdots dr_A \quad (3)$$

and

$$\langle \bar{r}_1 \bar{r}_2 | \Gamma_2 | \bar{r}_1' \bar{r}_2' \rangle = \frac{A(A-1)}{N} \int \Psi^*(\bar{r}_1, \bar{r}_2, \bar{r}_3, \dots, \bar{r}_A) \Psi(\bar{r}_1', \bar{r}_2', \bar{r}_3, \dots, \bar{r}_A) dr_3 \cdots dr_A, \quad (4)$$

with  $N$  being the normalization integral.

The structure of quantities (3) and (4) for an extended system of bosons in the presence of strong spatial correlations has been uncovered in a number of publications.<sup>10,14-21</sup> The formalism developed by Ristig and Clark provides powerful means for quantitative evaluation of the matrices (3) and (4) and related quantities as the momentum distribution, condensate fraction, pairing function, pairing energies, etc., for liquid  ${}^4\text{He}$ . Numerical results for those quantities have been published in Refs. 14-16 and 18.

This paper reports on the results of refined calculations of the one- and two-body density matrices of liquid  ${}^4\text{He}$ . Detailed results are presented to illuminate the dependence of the long-range order described by expressions (3) and (4) on density and, upon proper generalization, on temperature. The functions  $f(r)$  and the associated structure functions  $S(k)$  or, equivalently, the radial distribution functions  $g(r)$ , serve as inputs in the calculations performed. They have been obtained by carrying out a self-consistent paired-phonon analysis in conjunction with a hypernetted-chain (HNC) approximation.<sup>8</sup> The interatomic interaction is described by the Lennard-Jones (6-12) potential.

Our evaluation employs systematically the hypernetted-chain summation technique developed recently for the function

$$Q(r) = Q(0) - \ln \langle \bar{r}_1 | \Gamma_1 | \bar{r}_2 \rangle,$$

$r \equiv |\bar{r}_1 - \bar{r}_2|$  (see Ref. 21). This version of HNC procedure rests on the idea of series and parallel connection of diagrams which is familiar from the HNC scheme for the radial distribution function.<sup>12,22,23</sup>

The results presented for the condensate fraction of liquid  ${}^4\text{He}$  are in fair agreement with our earlier results which have been derived from the compact cluster expansion of Ristig and Clark truncated at low cluster order.<sup>16</sup> The new results on the density matrix and pairing function of liquid  ${}^4\text{He}$  improve significantly those of Refs. 16 and 18.

Adopting Schiff-Verlet's choice<sup>24</sup> for the correlation factor  $f(r)$  we find excellent agreement between the results of their molecular-dynamics treatment and our results for the pairing function. We are therefore convinced that the results of our present study provide reliable theoretical data on the coherent phenomena in liquid  ${}^4\text{He}$ .

Section II collects the formal results of the Ristig

and Clark analysis of the one-body density matrix and the pairing function. Fantoni's formulation of the HNC scheme for the one-body density matrix is summarized. Section III presents the results on the quantities of interest for describing condensation in liquid  ${}^4\text{He}$  and Sec. IV is devoted to the generalization of the formalism to finite temperatures. The condensate fraction of liquid  ${}^4\text{He}$  is studied as function of temperature.

## II. LONG-RANGE ORDER

The density matrices contain complete information on the properties of a many-body system. We can, for example, evaluate the kinetic energy if we know the one-body density matrix. Other physical quantities which are of interest are related to the two-body density matrix. The long-range behavior of both matrices gives direct information on the coherent effects of a quantum fluid.<sup>5</sup>

An approach which allows quantitative treatment of the functions (3) and (4) for a Bose fluid in its ground state described by Ansatz (2) has been developed in a series of publications.<sup>10,14,19,20</sup> The program carried through in these studies yielded important structural formulas for the one- and two-body density matrices and related quantities.

In this section we summarize the formal results which are needed for a description of the condensation phenomena in dense Bose fluids, in particular, liquid  ${}^4\text{He}$ . The formalism may serve as a basis for powerful and reliable approximation schemes which employ the HNC technique developed for the radial distribution function<sup>22</sup> and for the quantity

$$Q(r) - Q(0) = -\ln \langle \bar{r}_1 | \Gamma_1 | \bar{r}_2 \rangle$$

by Fantoni.<sup>21</sup>

The wave function (2) exhibits long-range order in the off-diagonal matrix elements of the one- and two-body density matrices,<sup>10,18,20</sup>

$$\lim_{|\bar{r}_1 - \bar{r}_1'| \rightarrow \infty} \langle \bar{r}_1 | \Gamma_1 | \bar{r}_1' \rangle = \rho n_c > 0, \quad (5)$$

$$\lim_{\substack{|\bar{r}_1 - \bar{r}_1'| \rightarrow \infty \\ r, r' < \infty}} \langle \bar{r}_1 \bar{r}_2 | \Gamma_2 | \bar{r}_1' \bar{r}_2' \rangle = f(r) n(r) f(r') n(r'), \quad (6)$$

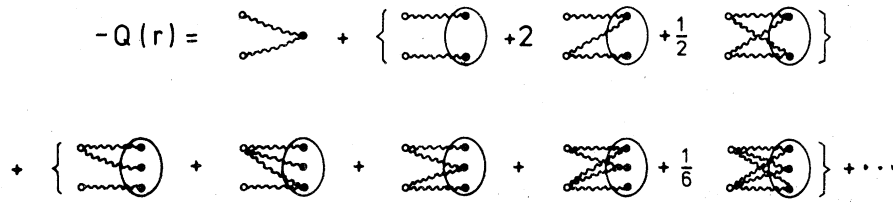


FIG. 1. Graphical representation of the function  $Q(r)$  in terms of successive distribution functions. The blob with two (three) points on it represents the two-(three)-body distribution function.

with

$$r = |\bar{r}_1 - \bar{r}_2|, \quad r' = |\bar{r}_1' - \bar{r}_2'|$$

Thus, the zero-momentum single-particle orbital is macroscopically occupied at any density  $\rho$ , the condensate fraction being given by quantity  $n_c$ . A strong correlation exists between the members of pairs of bosons with total momentum zero.<sup>17</sup> This coherent effect is appropriately described by the pairing function  $f(r)n(r)$ . Function  $n(r)$  is the density matrix (3) which has the structure<sup>10</sup>

$$\langle \bar{r}_1 | \Gamma_1 | \bar{r}_2 \rangle = n(r) = n_c e^{-Q(r)} \quad (7)$$

Quantity  $Q(r)$  and the fraction  $n_c$  have been extensively studied in Ref. 10. The function  $Q(r)$  is known as an expansion in terms of the successive distribution functions

$$g_2(\bar{r}_1, \bar{r}_2) \equiv g(r), \quad g_3(\bar{r}_1, \bar{r}_2, \bar{r}_3), \dots$$

Diagrammatically, quantity  $Q(r)$  may be represented by irreducible Ursell-Mayer cluster diagrams.<sup>10,23</sup> Figure 1 depicts the graphic representation of that function. The condensate fraction is given by

$$n_c = e^{Q(0)} \quad (8)$$

The exponent  $Q(0)$  may be written<sup>10</sup>

$$Q(0) = 2D[\zeta] - D[\eta] \quad (9)$$

where the functional  $D$  depends on the bare correlation factors

$$\zeta(r) = f(r) - 1, \quad \eta(r) = f^2(r) - 1 \quad (10)$$

Quantities (10) are represented graphically by wavy and dashed lines, respectively. (See Fig. 2.)

To perform partial summations of the expansions defining  $Q(r)$  and  $D$  it is best to represent the successive distribution functions

$$g_3(\bar{r}_1, \bar{r}_2, \bar{r}_3), \quad g_4(\bar{r}_1, \bar{r}_2, \bar{r}_3, \bar{r}_4), \dots$$

in terms of the radial distribution function  $g(r)$ .



FIG. 2. Same as Fig. 1, but for the functional  $D[\zeta]$ .

Function  $g_3(\bar{r}_1, \bar{r}_2, \bar{r}_3)$ , for example, is given in this scheme by the expansion shown in Fig. 3. The quantity  $g(r) - 1$  is graphically represented by a solid line.

The Iwamoto-Yamada expansion of function  $Q(r)$  in terms of the entities  $\zeta(r)$  and  $g(r) - 1$  may thus be written<sup>10</sup>

$$Q(r) = [\Delta Q(r)]^{[1]} + [\Delta Q(r)]^{[2]} + [\Delta Q(r)]^{[3]} + \dots \quad (11)$$

Here,  $[\Delta Q(r)]^{[n-2]}$  is the  $n$ -body cluster contribution which is represented by irreducible diagrams with two external and  $n - 2$  internal field points (Fig. 4).

Estimates of the function  $Q(r)$  for liquid <sup>4</sup>He have been reported in Ref. 16. The calculations are based on expansion (11) truncated at the four-body level. The apparent success of the HNC approximation in determining the radial distribution function<sup>23</sup> suggests strongly that one exploit the technique of series and parallel connection of diagrams to derive an analogous partial summation of expansion (11). This task has been successfully achieved in Ref. 21. In the following we summarize briefly the results for a system of bosons.

Let us begin with a structural decomposition of the Fourier inverse

$$Q(k) = \rho \int Q(r) e^{i\bar{k} \cdot \bar{r}} d\bar{r}, \quad (12)$$

$$-Q(k) = Q_1^2(k)S(k) + Q_E(k),$$

where  $S(k)$  is the liquid structure function<sup>12</sup> associated with Ansatz (2). The components

$$Q_1(r) = \rho^{-1} (2\pi)^{-3} \int Q_1(k) e^{i\bar{k} \cdot \bar{r}} d\bar{k}$$

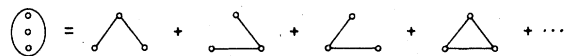
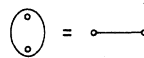


FIG. 3. Graphic representation of the three-body distribution function  $g(\bar{r}_1, \bar{r}_2, \bar{r}_3)$  in terms of the radial distribution function.

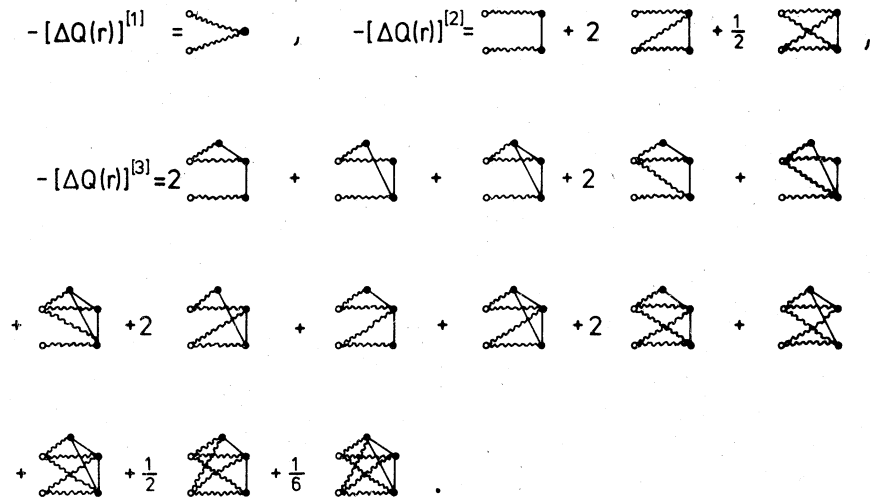


FIG. 4. Three-, four-, and five-body cluster contributions to function  $Q(r)$  in terms of functions  $\zeta(r)$  and  $g(r) - 1$ .

and

$$Q_E(r) = \rho^{-1} (2\pi)^{-3} \int Q_E(k) e^{i\vec{k}\cdot\vec{r}} d\vec{k}$$

may be represented by non-nodal and elementary diagrams, respectively. The leading cluster contributions to both functions are depicted in Fig. 5.

The function  $Q_1(r)$  obeys the HNC equations<sup>21</sup>

$$Q_1(r) = f(r) e^{Q_2(r) + Q_{2E}(r)} - Q_2(r) - 1, \quad (13)$$

$$Q_2(k) = Q_1(k) [S(k) - 1], \quad (14)$$

where quantity  $Q_2(r)$  collects the contributions of no-

$$D[\zeta] = \lim_{k \rightarrow 0^+} [Q_1(k) - Q_{2E}(k)] - (2\pi)^{-3} \frac{1}{2\rho} \int [Q_1(k) + Q_2(k)] [Q_2(k) + 2Q_{2E}(k)] d\vec{k} + E[\zeta]. \quad (15)$$

The functional  $E[\zeta] \equiv \hat{E}[Q_1]$  represents the contribution of elementary diagrams. The leading cluster term to this quantity is depicted in Fig. 6. The Fourier transforms of all quantities involved are defined in the same manner as shown explicitly for function  $Q_1(r)$ .

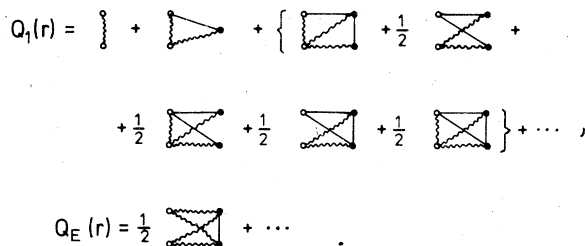


FIG. 5. Leading terms to the cluster expansions which define the functions  $Q_1(r)$  and  $Q_E(r)$ .

dal diagrams. Function  $Q_{2E}(r)$  may be characterized by elementary diagrams which have wavy lines attached to one external field point and solid lines to the other one. The corresponding cluster expansions are shown in Fig. 6.

Relations (13) and (14) permit a "dressing" of the bare correlation factor  $\zeta(r)$  in analogy to the well-known renormalization of function  $\eta(r)$  which yields the radial distribution function.

In a similar manner we may achieve a partial summation of the expansions defining the functionals  $D[\zeta]$  and  $D[\eta]$  which determine the condensate fraction (8) and (9). Fantoni gives the formula<sup>21</sup>

The analogous expression for functional  $D[\eta]$  may be generated from Eq. (15) by performing the replacement

$$Q_1(k) + Q_2(k) \rightarrow Q_1(k) S(k),$$

$$Q_1(k) \rightarrow [S(k) - 1]/S(k)$$

and  $\zeta(k) \rightarrow \eta(k)$ .

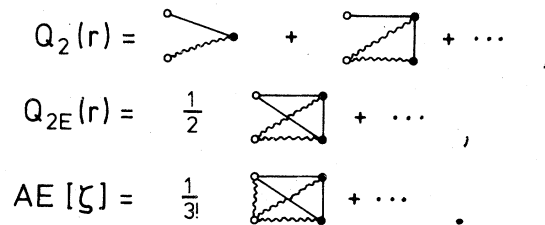


FIG. 6. Same as Fig. 5, but for quantities  $Q_2(r)$ ,  $Q_{2E}(r)$ , and  $E[\zeta]$ .

### III. BOSE-EINSTEIN CONDENSATION AND PAIR CONDENSATION

Numerical application of the formalism of Sec. II to describe the condensed phase of liquid  ${}^4\text{He}$  is based on the HNC equations (12)–(14) for the function  $Q(r)$  and the functional  $D$  given by Eq. (15). The procedure requires as inputs a suitable ground-state correlation factor  $f(r)$  and the associated spatial distribution function  $g(r)$  or the structure function

$$S(k) = 1 + \rho \int [g(r) - 1] e^{i\vec{k}\cdot\vec{r}} d\vec{r}.$$

Our main calculations employ the optimal Jastrow wave function (2), at the given particle density  $\rho$ , obtained by performing a paired-phonon analysis (PPA).<sup>8,12</sup> Numerical results are presented on the condensate fraction  $n_c$ , the pairing function  $f(r)n(r)$ , and related quantities for liquid  ${}^4\text{He}$  at the experimental saturation density  $\rho = 0.0218 \text{ \AA}^{-3}$ , and at higher densities up to densities in the solidification region ( $\rho \sim 0.026\text{--}0.028 \text{ \AA}^{-3}$ ). It should be mentioned that the paired-phonon model saturates at a density appreciably lower than the experimental value. However, there is no point in doing calculations at that lower density. We stress also that the model and experimental density scales are different.

The present improvement on the calculations of Ref. 16 lies in the incorporation of the hypernetted-chain diagrams into the approximation scheme for quantities  $Q(r)$  and  $D$ , which we did not consider in our earlier study. The HNC procedure adopted here begins with the HNC-0 approximation which omits the contributions of the elementary diagrams,

$$Q_E(r) = Q_{2E}(r) = E[\zeta] = E[\eta] \sim 0. \quad (16)$$

The next step of approximation includes the contributions from the basic four-point elementary diagrams. The resulting approximation is called HNC-4 in analogy to the procedure familiar from the treatment for the radial distribution function.<sup>23</sup>

For the functions of interest we find that the HNC-4 results do not differ significantly from the corresponding HNC-0 results. We believe therefore

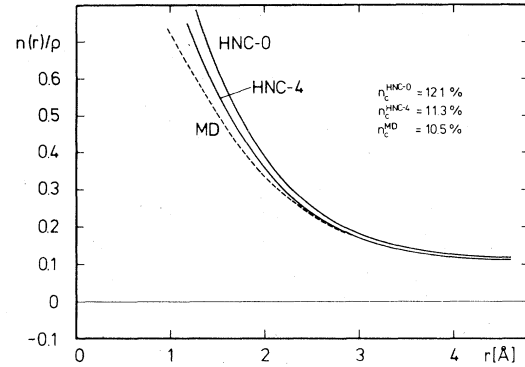


FIG. 7. One-body density matrix of liquid  ${}^4\text{He}$  at saturation density  $\rho = 0.0218 \text{ \AA}^{-3}$  for Schiff-Verlet choice of correlation factor, in HNC-0 and HNC-4 approximation. Curve MD depicts the result of Ref. 24 based on a molecular-dynamics treatment.

that the HNC scheme provides an accurate approximation for the quantities (5) and (6).

Our confidence is strongly supported by comparing the results of Schiff and Verlet<sup>24</sup> for the condensate fraction and one-body density matrix with those results derived by the HNC treatment. The calculation of Ref. 24 employs the trial correlation factor

$$f(r) = \exp \left[ -\frac{1}{2} \left( \frac{b}{r} \right)^5 \right], \quad (17)$$

with  $b = 2.965 \text{ \AA}$  at experimental equilibrium density of liquid  ${}^4\text{He}$ . Schiff-Verlet's results for the quantities in question are derived by a molecular dynamics technique and are shown in Table I, column MD, and Fig. 7, curve MD. For the same trial function (17) the HNC approximation adopted in present work yields the results called HNC-0 and HNC-4 in Table I and Fig. 7. The numerical results of differing approximations for quantity  $n_c$  are in fair agreement. Even the result of Ref. 16, based on the compact cluster expansion truncated at low cluster order, is quite good. The function  $f(r)n(r)$  vanishes for distances  $r \lesssim 2 \text{ \AA}$  since the correlation factor (17) is extremely small at such distances. We get, therefore, a

TABLE I. Condensate fraction of liquid  ${}^4\text{He}$  at experimental saturation density,  $\rho = 0.0218 \text{ \AA}^{-3}$ , and vanishing temperature, for Schiff-Verlet choice of correlation function (SV), Eq. (17), and in paired-phonon analysis (PPA).

$f(r)$	Ref. 16	HNC-0	HNC-4	MD <sup>a</sup>
SV	0.119	0.121	0.113	$0.105 \pm 0.005$
PPA	0.129	0.120	0.113	

<sup>a</sup>Results of Ref. 24 employing a molecular-dynamics method.

reliable result for the pairing function appearing in Eq. (6) if the one-body density matrix is known with sufficient accuracy for distances  $r > 2 \text{ \AA}$ . Indeed, Fig. 7 shows excellent agreement among the various approximations adopted for quantity  $n(r)$ ,  $r > 2 \text{ \AA}$ . Figure 8 demonstrates the rapid convergence of the successive HNC approximations for function  $Q(r)$  at density  $\rho = 0.0218 \text{ \AA}^{-3}$  with the optimal structure function as input. The results for the condensate fraction of liquid  ${}^4\text{He}$  at experimental saturation density obtained by performing a paired-phonon analysis are listed in Table I.

The condensate fraction is insensitive to the detailed form of correlation function  $f(r)$  at any density considered. The very short-range Schiff-Verlet or the long-range paired-phonon choice give essentially the same result (Fig. 9). Quantity  $n_c$  decreases with increasing density, the fraction being about 5% in the experimental solidification region. Several studies are available which support the possibility that a Bose-Einstein condensate might indeed be present in a quantum solid.<sup>7,25-27</sup> However, the simple Ansatz (2) presumably gives a very poor description of  ${}^4\text{He}$  in the solidification region.<sup>27</sup>

Information on the coherent effects associated with the off-diagonal long-range order of the two-body density matrix of liquid  ${}^4\text{He}$  is stored in the pairing function  $f(r)n(r)$  which may be interpreted as an average macroscopic field.<sup>20</sup> Figure 10 depicts that quantity as function of distance  $r$  in HNC-4 approximation corresponding to the optimal correlation factor  $f(r)$  at two differing densities, at the experimental saturation density, and at density  $\rho = 0.027 \text{ \AA}^{-3}$ . The pairing function approaches the value  $\rho n_c$  as  $r \rightarrow \infty$  and shows remarkable structure at intermediate distances. The amplitude of the oscillations appearing in the pairing function depends sensitively on the detailed form of correlation function  $f(r)$ . It is significantly larger in the paired-phonon than in the Schiff-Verlet model.

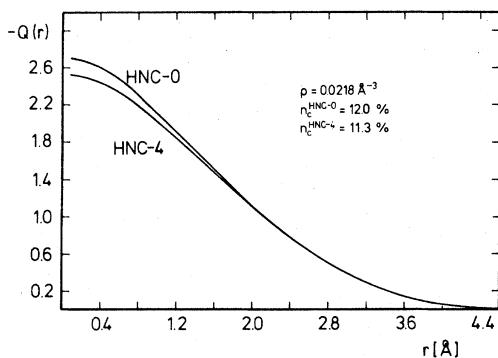


FIG. 8. Function  $Q(r)$  for liquid  ${}^4\text{He}$  at experimental saturation density in HNC-0 and HNC-4 approximation employing paired-phonon analysis.

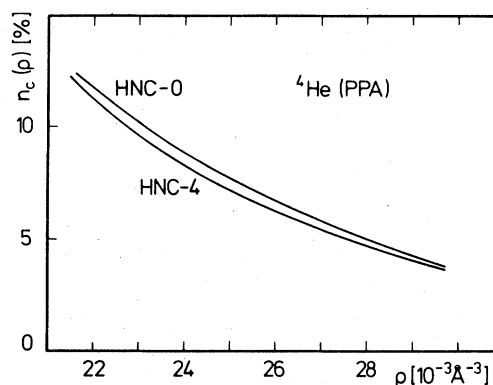


FIG. 9. Condensate fraction of liquid  ${}^4\text{He}$  as a function of density in HNC-0 and HNC-4 approximation employing the optimal Jastrow correlations.

An interesting portion of the ground-state energy of the fluid is the pairing energy<sup>18,20</sup>

$$E_P = -\frac{A}{2\rho} \int \Delta(r) f(r) n(r) d\bar{r}, \quad (18)$$

with the pairing potential

$$\Delta(r) = -v^*(r) f(r) n(r), \quad (19)$$

where quantity  $v^*(r)$  is the effective potential

$$V^*(r) = v(r) - \frac{\hbar^2}{2m} \Delta \ln f(r). \quad (20)$$

The interatomic potential  $v(r)$  is assumed to be of Lennard-Jones (6-12) type. Quantity  $E_P$  is that component of the expectation value of the ground-state energy with respect to the correlated wave function which is associated with boson pairs having zero total momentum.<sup>18</sup> Our results for the potential  $\Delta(r)$  are

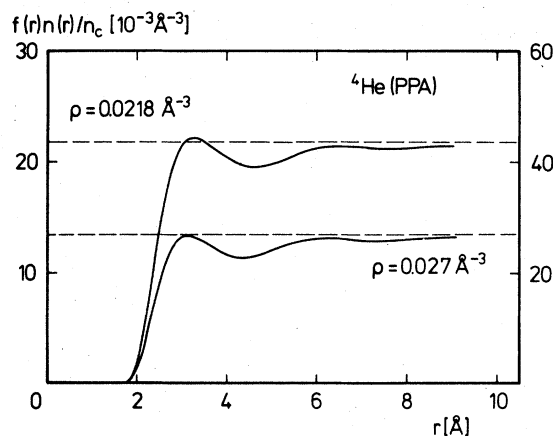


FIG. 10. Pairing function for liquid  ${}^4\text{He}$  in HNC-4 approximation based on optimal correlation factor, at two differing densities, left scale  $\rho = 0.0218 \text{ \AA}^{-3}$ , right scale  $\rho = 0.027 \text{ \AA}^{-3}$ .

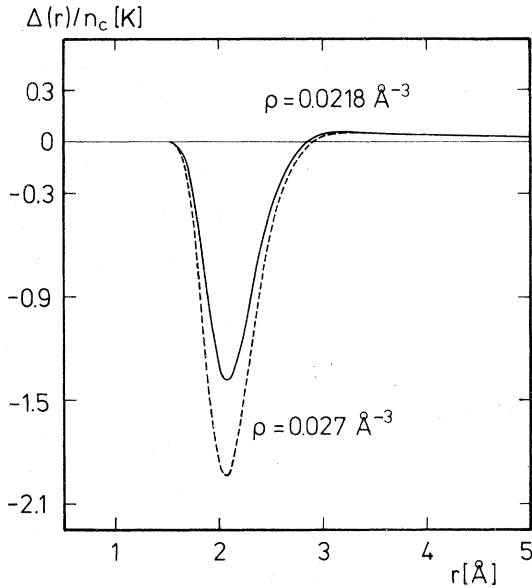


FIG. 11. Pairing potential of liquid  ${}^4\text{He}$  in HNC-4 approximation based on the PPA model at two differing densities.

represented in Fig. 11. The pairing potential is repulsive at small distances  $r \leq 3 \text{ \AA}$  and has a rather long attractive tail at intermediate distances.

It is worthwhile to express the pairing function and pairing potential by the Fourier transforms,

$$\chi(k) = - \int [f(r)n(r) - n_c\rho] e^{i\vec{k}\cdot\vec{r}} d\vec{r}, \quad (21)$$

and

$$\Delta(k) = \rho \int \Delta(r) e^{i\vec{k}\cdot\vec{r}} d\vec{r}, \quad (22)$$

respectively. Function (22) permits the energy (18) to be cast into the form

$$E_p = \frac{A}{2\rho} (2\pi)^{-3} \int [\Delta(k) - \Delta(0)] \chi(k) d\vec{k}. \quad (23)$$

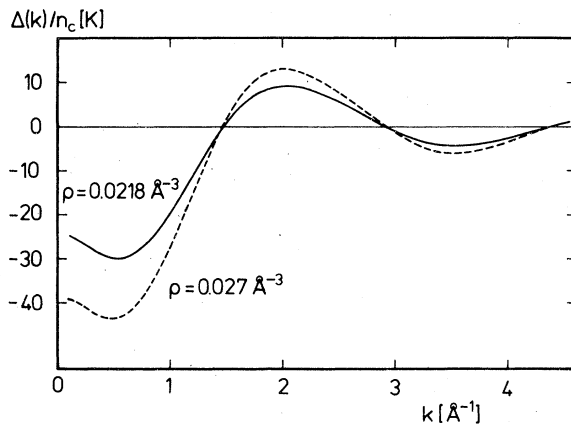


FIG. 12. Same as Fig. 11, but for quantity  $\Delta(k)$ .

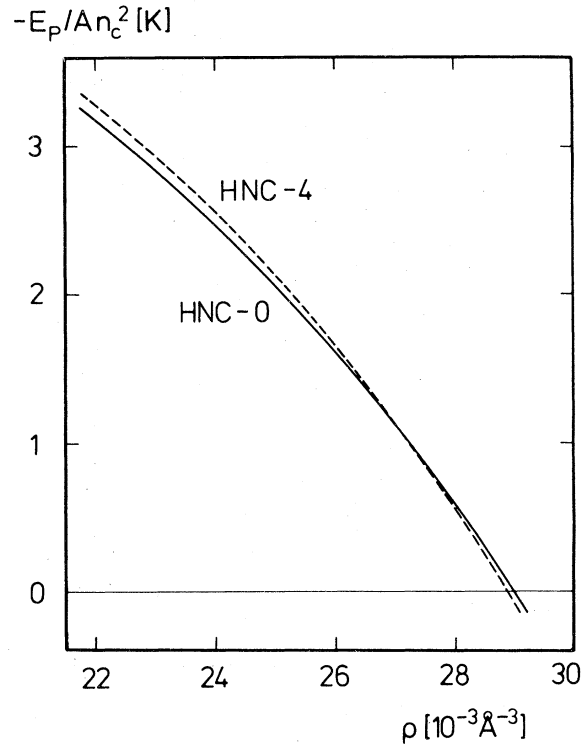


FIG. 13. Same as Fig. 9, but for pairing energy  $E_p/A$ .

Formulations (21)–(23) suggests a close analogy to the BCS treatment of superfluidity in the ground state of an extended system of fermions.<sup>28</sup> Figure 12 depicts the function  $\Delta(k)$  and its variation with density.

Insertion of our numerical results for the pairing function and pairing potential in Eq. (18) yields an estimate of the pairing energy in liquid  ${}^4\text{He}$  as function of density (Fig. 13). In the density range considered we find a negative value for the energy  $E_p$ , i.e., the attraction present in the pairing potential is sufficient to create a bound pair. The energy  $E_p/A$  of the boson pair in paired-phonon approximation is about 50 mK at saturation density and decreases rapidly with increasing density, becoming positive at density  $\rho \sim 0.029 \text{ \AA}^{-3}$ . The pairing energy corresponding to the Schiff-Verlet choice of correlation function shows a similar dependence on the density. However, the magnitude of quantity  $E_p/A$  is rather sensitive to the choice of the correlation function.

The close agreement between the results in HNC-0 and HNC-4 approximation (Fig. 13) suggests that the hypernetted-chain approach provides a reliable approximation scheme for the pairing energy of liquid  ${}^4\text{He}$ . Our results call clearly for an investigation of the effects of the boson pairing phenomenon on the excitation spectrum of liquid  ${}^4\text{He}$ .<sup>29</sup>

#### IV. CONDENSATE FRACTION AT LOW TEMPERATURE

Information on the condensate fraction of liquid  ${}^4\text{He}$  can be extracted from experimental data which are available from neutron scattering measurements.<sup>30</sup> Woods and Sears<sup>31</sup> have given a value  $n_c(T) = (6.9 \pm 0.8)\%$  for the condensate fraction at  $T = 1.1$  K. At present no measurements have been reported which allow one to draw definite conclusions about the dependence of the condensate on temperature.<sup>32</sup> Theoretical attempts on this problem have been made in Refs. 33 and 34. However, only the condensate fraction of the noninteracting Bose gas is known exactly,<sup>1</sup>

$$n_0(T) = 1 - (T/T_c)^{3/2}. \quad (24)$$

The condensate vanishes at the transition temperature  $T_c$ . For a system of interacting bosons models have been developed which rest on the assumption that certain types of elementary excitations exist at finite temperatures propagating freely through the liquid.

The paired-phonon model developed by Feenberg<sup>35</sup> assumes that the elementary excitations in liquid  ${}^4\text{He}$  are phonons and rotons which do not scatter, coalesce, or split. They may be described by the Bijl-Feynman excitation spectrum<sup>12</sup>

$$\epsilon(k) = \frac{\hbar^2 k^2}{2mS(k)}. \quad (25)$$

It is possible to generalize the paired-phonon model appropriately to take account of a substantial part of the effects generated by the interaction between and among the elementary excitations.<sup>35</sup>

Adopting Feenberg's model for a description of liquid  ${}^4\text{He}$  at finite temperatures the condensate fraction may be evaluated from<sup>36</sup>

$$n_c(T) = e^{-(T/T_0)^{2/8}} e^{Q(T)}. \quad (26)$$

For vanishing temperature, expression (26) reduces to the formula (8) discussed in Sec. II. The temperature  $T_0$  is defined as

$$T_0 = [\rho(\hbar s)^3 / ms^2 k_B^2]^{1/2},$$

with the velocity of ordinary sound  $s$  and Boltzmann constant  $k_B$ . At saturation density  $\rho = 0.0218 \text{ \AA}^{-3}$  we find the value  $T_0 = 2.195$  K. Quantity  $Q(T)$  can be viewed as an appropriate generalization of Eq. (9) to finite temperatures,<sup>36</sup>

$$Q(T) = 2D_T[\zeta(T)] - D_T[\eta(T)]. \quad (27)$$

The functionals  $D_T$  and  $D$ , appearing in Eqs. (9) and

(27), have the same graphic representation (Fig. 2). However, the ingredients (10) which are depicted by wavy and dashed lines are dependent on temperature and derive from a correlation factor<sup>36</sup>

$$f(r, T) = f(r) f_{\text{th}}(r, T), \quad (28)$$

$$\rho \ln f_{\text{th}}(r, T) = \int \frac{e^{i\vec{k}\cdot\vec{r}} d\vec{k}}{S(k) \{\exp[\epsilon(k)/k_B T] + 1\}}. \quad (29)$$

Expression (28) describes the optimal ground-state correlations as well as the thermal correlations present at finite temperatures. The solid line represents the radial distribution function which is associated with the correlation factor (28). Exploiting separability in the paired-phonon analysis it may be shown<sup>35</sup> that the corresponding temperature-dependent structure function has the simple form

$$S(k, T) = S(k) \coth[\frac{1}{2} \epsilon(k)/k_B T]. \quad (30)$$

The paired-phonon model just described should provide a good approximation for the condensate fraction of liquid  ${}^4\text{He}$  at temperatures  $T \leq 1.5$  K.<sup>35</sup> Of course, if scattering, coalescing, and splitting of phonons and rotons become important or other types of elementary excitations appear in liquid  ${}^4\text{He}$  the adopted model is no longer valid and must be properly reformulated.

A preliminary numerical evaluation of the condensate fraction for liquid  ${}^4\text{He}$  at low temperatures has been reported in Ref. 36. The calculation was based on the Iwamoto-Yamada cluster expansion for the function  $Q(T)$  truncated at the four-body cluster level [cf. Eq. (13) of Ref. 36]. Applying the HNC formalism with the correlation factor (28) as input, we have evaluated quantity (27) in HNC-0 and HNC-4 approximation as described in Secs. II and III.

Table II presents our refined results for the condensate fraction  $n_c(T)$  at the experimental saturation density. The HNC results do not alter the qualitative behavior of our earlier results observed in Ref. 36.

TABLE II. Condensate fraction of liquid  ${}^4\text{He}$  at experimental saturation density as function of temperature based on the paired-phonon model.

$T$ (K)	HNC-0	HNC-4
0	0.120	0.113
1.0	0.119	0.112
1.4	0.116	0.109
1.8	0.113	0.107
2.2	0.111	0.104



The condensate fraction depends very weakly on temperature. The model adopted limits the validity of our calculation for liquid  $^4\text{He}$  to temperatures below  $T = 1.5$  K. At higher temperatures an adequate description of liquid  $^4\text{He}$  should reflect that the condensate fraction vanishes at the superfluid transition temperature. The expected behavior is not reproduced by the model adopted. In contrast, the function  $n_c(T)$  remains almost independent of tem-

perature signaling the breakdown of the paired-phonon model in the critical region.

#### ACKNOWLEDGMENT

This research was supported in part by the Deutsche Forschungsgemeinschaft under Grant No. Ri 267/3/4.

- 
- <sup>1</sup>F. London, *Superfluids* (Wiley, New York, 1954).  
<sup>2</sup>C. E. Campbell, in *Progress in Liquid Physics*, edited by C. A. Croxton (Wiley, New York, 1978).  
<sup>3</sup>C. W. Woo, in *The Physics of Liquid and Solid Helium*, edited by K. H. Bennemann and J. B. Ketterson (Wiley, New York, 1976), Vol. I.  
<sup>4</sup>R. M. Ziff, G. E. Uhlenbeck, and M. Kac, *Phys. Rep. C* **32**, 170 (1977).  
<sup>5</sup>C. N. Yang, *Rev. Mod. Phys.* **34**, 694 (1962).  
<sup>6</sup>E. Feenberg, *Ann. Phys. (N.Y.)* **84**, 128 (1974).  
<sup>7</sup>L. Reatto, *Rivista Nuovo Cimento* **5**, 108 (1975).  
<sup>8</sup>C. C. Chang and C. E. Campbell, *Phys. Rev. B* **15**, 4238 (1977).  
<sup>9</sup>L. Reatto, *Phys. Rev.* **183**, 334 (1969).  
<sup>10</sup>M. L. Ristig and J. W. Clark, *Phys. Rev. B* **14**, 2875 (1976).  
<sup>11</sup>H. W. Jackson, *Phys. Rev. A* **10**, 278 (1974).  
<sup>12</sup>E. Feenberg, *Theory of Quantum Fluids* (Academic, New York, 1969).  
<sup>13</sup>L. J. Lantto, A. D. Jackson, and P. J. Siemens, *Phys. Lett. B* **68**, 311 (1977).  
<sup>14</sup>M. L. Ristig, P. M. Lam, and J. W. Clark, *Phys. Lett. A* **55**, 101 (1975).  
<sup>15</sup>P. M. Lam and C. C. Chang, *Phys. Lett. A* **59**, 356 (1976).  
<sup>16</sup>P. M. Lam, J. W. Clark, and M. L. Ristig, *Phys. Rev. B* **16**, 222 (1977).  
<sup>17</sup>M. L. Ristig, *Phys. Lett. A* **58**, 390 (1976).  
<sup>18</sup>M. L. Ristig, P. Hecking, P. M. Lam, and J. W. Clark, *Phys. Lett. A* **63**, 94 (1977).  
<sup>19</sup>M. L. Ristig, *Phys. Rev. B* **18**, 1207 (1978).  
<sup>20</sup>M. L. Ristig, *Nucl. Phys. A* (to be published).  
<sup>21</sup>S. Fantoni, *Nuovo Cimento A* **44**, 191 (1978).  
<sup>22</sup>J. M. J. van Leeuwen, J. Groeneveld, and J. de Boer, *Physica (Utrecht)* **25**, 792 (1959).  
<sup>23</sup>J. W. Clark, in *Progress in Particle and Nuclear Physics*, edited by D. H. Wilkinson (Pergamon, Oxford, 1979), Vol. II.  
<sup>24</sup>D. Schiff and L. Verlet, *Phys. Rev.* **160**, 208 (1967).  
<sup>25</sup>G. V. Chester, *Phys. Rev. A* **2**, 256 (1970).  
<sup>26</sup>J. F. Fernandez and H. A. Gersch, *Phys. Rev. A* **7**, 239 (1973).  
<sup>27</sup>J. P. Hansen and E. L. Pollock, *Phys. Rev. A* **5**, 2651 (1972).  
<sup>28</sup>J. R. Schrieffer, *Theory of Superconductivity* (Benjamin, New York, 1964).  
<sup>29</sup>R. Hastings and J. W. Halley, *Phys. Rev. B* **12**, 267 (1975).  
<sup>30</sup>A. D. B. Woods and R. A. Cowley, *Rep. Prog. Phys.* **36**, 1135 (1973).  
<sup>31</sup>A. D. B. Woods and V. F. Sears, *Phys. Rev. Lett.* **39**, 415 (1977).  
<sup>32</sup>H. J. Raveché and R. D. Mountain, *Phys. Rev. A* **9**, 435 (1974).  
<sup>33</sup>G. J. Hyland, G. Rowlands, and F. W. Cummings, *Phys. Lett. A* **31**, 465 (1970).  
<sup>34</sup>G. J. Hyland and G. Rowlands, *Phys. Lett. A* **62**, 154 (1977).  
<sup>35</sup>E. Feenberg, *Ann. Phys. (N.Y.)* **70**, 133 (1972).  
<sup>36</sup>P. M. Lam and M. L. Ristig, *Phys. Lett. A* **65**, 307 (1978).